A bacterial effector protein hijacks plant metabolism to support bacterial nutrition

Liu Xian[1,2,3], Gang Yu[1,3], Yali Wei[1,2], Jose S. Rufian[1], Yansha Li[1], Haiyan Zhuang[1], Hao Xue[1,2], Rafael J. L. Morcillo[1], and Alberto P. Macho[1,*].

[1]Shanghai Center for Plant Stress Biology, CAS Center for Excellence in Molecular Plant Sciences; Shanghai Institutes of Biological Sciences, Chinese Academy of Sciences, Shanghai 201602, China.

[2]University of Chinese Academy of Sciences, Beijing, 100049, China.

[3]These authors contributed equally to this work.

*Corresponding author: alberto.macho@sibs.ac.cn

Summary

Most bacterial plant pathogens inject effector proteins inside plant cells, using a type-III secretion system, to suppress plant immunity. However, whether and how effector proteins co-opt plant metabolism to produce nutrients that support extensive bacterial replication is not understood. In this work, we found that *Ralstonia solanacearum*, the causal agent of bacterial wilt disease, secretes an effector protein, named RipI, which interacts with plant glutamate decarboxylases (GADs). GADs catalyse the biosynthesis of GABA, an important signalling molecule in plants and animals, and are activated by calmodulin. RipI promotes the interaction of GADs with calmodulin, enhancing the production of GABA. Interestingly, *R. solanacearum* is able to replicate efficiently using GABA as a nutrient, and both RipI and plant GABA contribute to a successful infection. This reveals a pathogenic strategy to hijack plant metabolism for the biosynthesis of nutrients to support microbial growth during plant colonization.

Keywords

Ralstonia; effector; GABA; virulence; nutrition; metabolism; calmodulin; GAD

Introduction

Diseases caused by bacterial pathogens are a threat to food security. *R. solanacearum* is a soil-borne bacterial pathogen able to cause disease in more than 250 plant species, including important crop plants, such as tomato, potato, pepper, and banana, causing serious losses to crop production worldwide (Elphinstone, 2005). Upon penetration into roots, *R. solanacearum* colonizes xylem vessels in host plants and replicates massively, ultimately causing plant wilting and death (Genin, 2010; Xue et al, 2020). Like other gram-negative bacterial pathogens, *R. solanacearum* requires a type-III secretion system to inject effector proteins inside host cells and cause disease. The activity of type-III effectors (T3Es) in the suppression of plant immunity has been well documented (Macho and Zipfel, 2015) (Toruño et al., 2016), although much less is known about the manipulation of the host microenvironment to support pathogenic lifestyle (Macho, 2016). The foliar bacterial pathogens *Pseudomonas syringae* and *Xanthomonas gardneri* use T3Es to increase the intercellular humidity in the leaf apoplast (Schwartz et al., 2017; Xin et al., 2016). Moreover, T3Es from *Xanthomonas* spp. induce the expression of host sugar transporters, likely causing an efflux of sugar to feed bacteria in the xylem or the apoplast (Chen et al., 2010; Cohn et al., 2014; Cox et al., 2017). Upon bacterial perception, defence responses include a restriction of nutrient transfer from the cytosol to the apoplast to limit bacterial multiplication (Chen et al., 2010; Wang et al., 2012; Yamada et al., 2016), suggesting that the battle for nutrient biosynthesis and distribution is essential for the outcome of plant-bacteria interactions. Similarly, although the xylem sap is generally poor in organic carbon sources compared to the phloem or the leaf apoplast (Fatima and Senthil-Kumar, 2015; Rico and Preston, 2008; Zuluaga et al., 2013), *R. solanacearum* is able to replicate very fast and reach high cell densities, implying the presence of additional virulence activities to subvert host nutrient metabolism or transport.

R. solanacearum secretes more than 70 T3Es into plant cells (Peeters et al., 2013; Sabbagh et al., 2019). This number is significantly higher than the usual number of

T3Es existing in other well-studied bacterial pathogens (15-40 in strains of *P. syringae* or *Xanthomonas*). The variety of T3Es utilized by *R. solanacearum* correlates with its broad ecological diversity, versatility, and ability to colonize different plant organs, such as roots, stems and leaves. Interestingly, several of these T3Es do not present homologs in other pathogens, which suggests that they have evolved exclusively in *R. solanacearum* (Peeters et al., 2013; Sabbagh et al., 2019). One of these exclusive T3Es, RipI, is conserved in most sequenced *R. solanacearum* strains (Peeters et al., 2013), which suggests its importance for bacterial virulence, although its actual contribution to the infection has not yet been determined and characterized. In this work, we found that RipI has a significant contribution to the development of disaese in both *Arabidopsis thaliana* (hereafter, Arabidopsis) and tomato plants. We show that RipI interacts with plant glutamate decarboxylases to cause an elevation of GABA, and that *R. solanacearum* can use this aminoacid as a nutrient during the infection, revealing a pathogenic strategy to manipulate plant metabolism to support bacterial nutrition.

Results and Discussion

RipI contributes to virulence in *Ralstonia solanacearum*

RipI is conserved in most sequenced *R. solanacearum* strains (Peeters et al, 2013), especially in strains isolated from tomato (Sabbagh et al., 2019). Since T3E activities often contribute redundantly to the development of disease, it is generally difficult to determine their contribution to virulence. To determine the importance of RipI for the induction of disease by *R. solanacearum*, we generated a *ΔripI* knockout mutant strain using the reference GMI1000 strain as background (Figures S1A and S1B). The *ΔripI* mutant strain caused delayed and weaker disease symptoms compared to wild-type (WT) bacteria upon soil-drenching inoculation of Arabidopsis plants (Figures 1A, 1B, S1C, and S1D). A slight symptom attenuation was observed upon soil-drenching inoculation of tomato plants (Figures S1E-H), a natural host of *R. solanacearum*. To perform a more accurate assessment of disease development in tomato, we injected tomato stems with WT or the *ΔripI* knockout mutant, and observed that the mutation of *ripI* caused a significant reduction in bacterial replication in the xylem (Figure 1C), indicating that RipI is contributes to the proliferation of *R. solanacearum* in the xylem of host plants. In all cases, the virulence attenuation of the *ΔripI* mutant was rescued by the additional expression of *ripI* in bacterial cells (Figures 1A-C,and S1C-H). These results indicate that, among the *R. solanacearum* T3E repertoire, *ripI* plays a significant role in virulence.

RipI interacts with calmodulins and glutamate decarboxylases

To identify potential plant targets of RipI, we expressed RipI fused to a C-terminal GFP tag (RipI-GFP) in *Nicotiana benthamiana* using *Agrobacterium tumefaciens*. Then we immunoprecipitated RipI-GFP and analyzed interacting proteins using liquid chromatography followed by tandem mass-spectrometry (LC-MS/MS). Among RipI-associated proteins, we identified calmodulins (Figure S2A). We also identified calmodulins as interactors of RipI in a yeast-two-hybrid (Y2H) screen using a library of cDNA from tomato plants inoculated with *R. solanacearum* (Figure S2B). We

validated the interaction of RipI with endogenous plant calmodulins upon transient expression in *N. benthamiana* by pull-down using a calmodulin-binding resin (Figure 2A). Among the proteins that physically associate with RipI in plant cells, we identified the *N. benthamiana* ortholog of the Arabidopsis GLUTAMATE DECARBOXYLASE 4 (AtGAD4) (Figure S2A). GADs are enzymes that catalyse the biosynthesis of gamma-aminobutyric acid (GABA) from glutamic acid (Figure S2C) and, in plants, their activity is stimulated by calmodulin binding (Baum et al., 1996) (Snedden et al., 1996). *GAD*s form a gene family with several members in Arabidopsis, *N. benthamiana*, and tomato (Figure S2D). When trying to perform targeted co-immunoprecipitation to validate the interaction between RipI and GADs transiently expressed in *N. benthamiana*, we noticed that RipI expression inhibited the simultaneous *A. tumefaciens*-mediated expression of other genes (Figure S3). Therefore, we expressed different GADs in *N. benthamiana* cells and subsequently expressed RipI using an estradiol (EST)-inducible promoter (Figure S4A). Co-immunoprecipitation confirmed that RipI interacts with several GADs from different plant species *in planta*, including AtGAD1, AtGAD2, AtGAD4, NbGAD4, and SlGAD2 (Figure 2B). We observed a similar result by *in vitro* pull-down using RipI fused to a maltose-binding protein (MBP) tag produced and purified from *Escherichia coli* and AtGAD4 purified from *N. benthamiana* (Figure S4B). Additionally, we validated the direct interaction of RipI with GADs *in planta* by Förster resonance energy transfer – fluorescence lifetime imaging (FRET-FLIM) (Figures 2C and S3C).

RipI enhances GABA accumulation in plant cells through promoting calmodulin binding to GADs

GABA is a four-carbon non-proteinogenic amino acid that was first isolated from plant extracts prior to its characterization as a major neurotransmitter in animals. GABA was first defined as a carbon-nitrogen metabolite in plants, although increasing evidence demonstrates that it also plays an important role as signalling molecule (Ramesh et al., 2017). Since RipI associates with plant GADs, we sought to determine whether RipI has an impact in GABA accumulation in the plant. Strikingly,

GABA levels increased 50-fold in *N. benthamiana* tissues 2 days upon transient expression of RipI (Figure 3A). This effect was not observed upon expression of INF1, a heterologous elicitor of immunity and cell death from the oomycete pathogen *Phytophthora infestans* (Kamoun et al., 1998) (Figure 3A). Similarly, Arabidopsis transgenic lines expressing an EST-inducible RipI showed enhanced accumulation of GABA (Figures S5A-B). Glutamic acid levels showed only a minor reduction in *N. benthamiana* tissues expressing RipI (Figure S5C), suggesting that metabolic rearrangements may compensate for the enhanced GAD-mediated GABA biosynthesis. Interestingly, GABA has been shown to inhibit the pathogenicity of *A. tumefaciens* (Chevrot et al., 2006), which may explain our difficulties to perform transient co-expression of RipI and other genes using *A. tumefaciens* (Figure S3). Moreover, GABA can act as a stress signal in plants (Shelp et al., 2012), and stable transgenic plants that over-accumulate GABA are not viable (Koike et al., 2013). It is noteworthy that sustained expression of RipI in *N. benthamiana* or tomato using *A. tumefaciens* led to the appearance of cell death 4-5 days after *A. tumefaciens* inoculation (Figures S5D-S5G). Moreover, transgenic Arabidopsis plants constitutively expressing RipI died soon after germination, and EST-inducible RipI expression strongly inhibited seedling growth (Figure S5H). Interestingly, the expression of RipI induces apoptosis in yeast cells (Deng et al., 2016), suggesting that this effector has a toxic effect in eukaryotic cells. Although these observations suggest that the enhanced GABA accumulation caused by RipI may underlie the development of cell death upon sustained RipI expression, sustained expression of AtGAD4 in *N. benthamiana* caused a strong increase in GABA accumulation (Figure 3A) but no cell death (Figures S5I and S5J). Therefore, the cell death induced by RipI in eukaryotic cells seems to be caused by other activity (or activities) independent of, or in addition to, the enhancement of GABA accumulation, and remains to be determined.

RipI associates with both GADs and calmodulin (Figure 2), and the activity of plant GADs is stimulated by calmodulin binding (Baum et al., 1996) (Snedden et al., 1996).

Interestingly, RipI enhanced the interaction between endogenous calmodulin and GADs in Arabidopsis cells (Figures 3B, 3C, and S5K), suggesting that the RipI-mediated increase in GABA accumulation in plant cells is caused by an enhancement of GAD activity by the stimulation of calmodulin binding. In support of this hypothesis, RipI did not enhance GABA accumulation in *N. benthamiana* tissues undergoing virus-induced gene silencing (VIGS) of *NbCaM2* (*CALMODULIN 2*) (Figures 3D, S5L and S5M), indicating that RipI needs NbCAM2 to enhance GAD activity in *N. benthamiana*.

GABA can be used as a nutrient by *R. solanacearum*

GABA is abundant in the xylem of tomato plants and can be rapidly consumed by *R. solanacearum* (Zuluaga et al., 2013). Interestingly, the fungal pathogen *Cladosporium fulvum* enhances GABA production in infected plants and is able to use GABA as a nutritional source (Solomon and Oliver, 2002). Considering this, it was previously hypothesized that pathogens may alter plant metabolism to induce the accumulation of GABA and, potentially, other compounds to support bacterial nutrition (Zuluaga et al., 2013) (Solomon and Oliver, 2002) (Ward et al., 2010). GABA levels also increase upon plant inoculation with the pathogenic bacteria *P. syringae* pv. tomato (*Pto*) DC3000, but not upon inoculation with a non-pathogenic strain (Ward et al., 2010), and this metabolite has been shown to be a nutritional substrate for *Pto* DC3000 *in vitro* (Rico and Preston, 2008). However, alternative observations led to the hypothesis that *Pto* DC3000 degrades plant GABA to avoid toxic effects for bacterial cells (Park et al., 2010). In order to determine the effect of GABA on *R. solanacearum in vitro*, we first incubated *R. solanacearum* in minimal medium (MM) with or without the addition of GABA as sole nutrient. *R. solanacearum* did not replicate significantly in MM, but replicated to high levels in the presence of 5 mM GABA (Figures 4A and 4B), consistent with the fast rate of GABA consumption observed for *R. solanacearum* (Zuluaga et al., 2013). Similar results were obtained when incubating *R. solanacearum* in 10% rich medium or xylem sap extracted from tomato plants

198 (Figures S6A-D). Altogether, these results confirm that GABA can be used by *R.*
199 *solanacearum* as a nutrient.
200
201 **Plant GABA contributes to *R. solanacearum* infection**
202 In order to determine if *R. solanacearum* needs plant GABA for infection, we first used
203 Arabidopsis plants carrying mutations in *AtGAD1* and *AtGAD2* (*gad1/2*), which
204 accumulate significantly less GABA than WT plants before and after inoculation with
205 *R. solanacearum* (Mekonnen et al., 2016) (Figure S6E). Upon soil-drenching
206 inoculation, *R. solanacearum* caused weaker and delayed disease symptoms in
207 *gad1/2* mutant plants (Figures 5A, 5B, S6F, and S6G), and plant colonization,
208 measured as bacterial numbers in aerial tissues, was also compromised in *gad1/2*
209 mutant plants (Figure S6H). It is noteworthy that *gad1/2* mutant plants did not show
210 enhanced resistance to *Pto* DC3000 (Figure 5C), suggesting that other bacterial
211 pathogens may not rely on plant GABA to cause disease. To determine the
212 requirement of GABA during the infection of a natural host, we performed
213 RNAi-mediated silencing in tomato roots to reduce the expression of the most highly
214 expressed tomato *GAD* gene, *SlGAD2* (Figure S6I). Tomato plants harbouring roots
215 with reduced *GAD2* expression showed enhanced resistance to wilt symptoms upon
216 soil-drenching inoculation with *R. solanacearum* (Figures 5D-F, S6J-L). Altogether,
217 these results indicate that plant GABA contributes to *R. solanacearum* infection.
218 Interestingly, the *ΔripI* mutant strain did not show additional virulence attenuation in
219 *gad1/2* plants (Figures 5G, 5H, S6M and S6N). This result suggests that the
220 enhancement of GAD-mediated GABA production is the major virulence activity of
221 RipI, although it is worth considering that minor additional reductions in virulence may
222 not be detected due to the lack of sensitivity of this assay to detect small differences in
223 weak disease symptoms. Since *R. solanacearum* consumes plant GABA and RipI
224 induces GABA production, we reasoned that plants undergoing an infection by a *ΔripI*
225 mutant (which can consume GABA but lacks the RipI activity to induce GABA
226 production) would accumulate less GABA than plants undergoing an infection with *R.*
227 *solanacearum* GMI1000. Indeed, plants inoculated with a *ΔripI* mutant showed a

slight (reproducible but not statistically significant) reduction in GABA contents compared to those inoculated with *R. solanacearum* GMI1000 (Figure S6O); however, the interpretation of this result may be hindered by the large variation in GABA measurements among inoculated plants, and the fact that the replication of the *ΔripI* mutant in plant tissues is strongly compromised (Figure 1C), and this could lead to a weaker GABA consumption in these plants.

Numerous bacterial species produce proteins annotated as GADs, including *Cupriavidus campinensis* (sequence identifier: WP_144198345), which, as *R. solanacearum*, belongs to the *Burkholderiaceae* family. Strikingly, we did not find any genes among *R. solanacearum* genomes annotated as GADs or showing significant similarity to plant or bacterial GADs (see methods). The absence of endogenous GAD enzymes may be related to the necessity of *R. solanacearum* to utilize plant GABA for a fully successful infection (Figure 5). Many bacterial species also contain GABA transaminases, which mediate GABA catabolism; *gabT* genes, encoding GABA transaminases, are in fact required to utilize exogenous GABA in *P. syringae* (Park et al., 2010), which otherwise also lacks annotated GADs. The *R. solanacearum* genome contains a single gene encoding a GABA transaminase (*gabT*), which we mutated to study the importance of GABA utilization for *R. solanacearum* infection (Figures S1I and S1J). Unlike WT *R. solanacearum*, the *ΔgabT* knockout mutant was unable to grow in MM with GABA (Figure 6A), and showed a dramatic reduction in its ability to cause disease symptoms in Arabidopsis upon soil drenching inoculation (Figures 6B and 6C, S6P, and S6Q) and to grow in tomato upon stem injection (Figure 6D), suggesting that *R. solanacearum* requires the GabT transaminase to utilize GABA, and that this is essential to cause disease. The *ΔgabT* mutant strain did not show further virulence attenuation in *gad1/2* mutant plants (Figures 6E, 6F, S6R, and S6S), suggesting that its virulence attenuation is indeed associated to its inability to process plant GABA.

GADs as susceptibility factors during *R. solanacearum* infection

Our results indicate that plant GABA contributes to *R. solanacearum* infection, rather than being involved in plant defence against this pathogen. In keeping with this notion, *GAD* genes are up-regulated in different susceptible hosts in comparison with resistant plants upon *R. solanacearum* infection (Figure S7). How may *R. solanacearum* benefit from the conversion of one potential nutritional source (glutamate) into another (GABA)? It is possible that, by promoting the synthesis of GABA, *R. solanacearum* avoids competition with other plant metabolic pathways that use a versatile substrate such as glutamate. This is reminiscent of the strategy employed by *A. tumefaciens*, which subverts plant metabolism to promote the production of opines, an unusual exclusive nutrient that this pathogen is particularly equipped to use (Subramoni et al., 2014). Moreover, given the unclear effect of GABA on certain pathogens such as *P. syringae* (Ward et al., 2010) (Park et al., 2010) (Figure 5C), and its effect on inhibiting the virulence of others, such as *A. tumefaciens* (Chevrot et al., 2006) (Figure S3), we should consider the possibility that, in natural conditions, the RipI-mediated enhancement of GABA production may help *R. solanacearum* to gain nutrients while countering potential competing microorganisms. It is noteworthy that GABA accumulation is significantly different in different plant species: for example, while GABA is very abundant in most organs in tomato, including the xylem (Zuluaga et al., 2013; Ramesh et al., 2017), GABA levels are very low in Arabidopsis plants, although they have been reported to increase in response to infection (Tarkowski et al., 2020). Interestingly, we have found that RipI contributes to disease in both Arabidopsis and tomato (Figure 1), and GADs are required for full susceptibility against *R. solanacearum* in these plant species (Figure 5), suggesting that, even at different absolute concentrations, the relative abundance of GABA is important for *R. solanacearum* infection.

Our findings reveal a pathogenic strategy to hijack plant metabolism for the biosynthesis of nutrients to support the dramatic microbial growth that takes place during plant colonization by *R. solanacearum*. Considering the contribution of RipI, GabT, and plant GABA to *R. solanacearum* infection, this process seems to play an

288 important role in the development of bacterial wilt disease. As a consequence, GADs
289 emerge as plant susceptibility factors during *R. solanacearum* infection, paving the
290 way for the development of strategies to generate resistance against bacterial
291 diseases.
292

Acknowledgements

We thank Nemo Peeters and Anne-Claire Cazale for sharing unpublished biological materials, Axel Mithöfer and Jianru Zuo for sharing biological materials, Rosa Lozano-Duran for critical reading of this manuscript, Achen Zhao, Junyu Chen and Xue Zhang for technical assistance, and Xinyu Jian for technical and administrative assistance during this work. We thank the PSC Cell Biology and Proteomics core facilities for assistance with confocal microscopy and LC-MS/MS analysis, respectively. This work was supported by the Strategic Priority Research Program of the Chinese Academy of Sciences (grant XDB27040204), the National Natural Science Foundation of China (NSFC; grant 31571973), the Chinese 1000 Talents Program, and the Shanghai Center for Plant Stress Biology (Chinese Academy of Sciences). The authors have no conflict of interest to declare.

Author contributions

L.X. and G.Y. carried out most of the experiments and analysed data; Y.W. and Y.L. purified recombinant proteins and performed *in vitro* interaction assays; H.X. and J.S.R. generated *Ralstonia* mutant strains; J.S.R. and H.Z. performed additional experiments for the manuscript revision; R.J.L.M. performed tomato root transformation; A.P.M. and L.X. initiated the project and designed the experiments; A.P.M. analysed data and supervised the project; A.P.M., L.X., and G.Y. wrote the manuscript with inputs from all the authors.

Declaration of interests

The authors declare no competing interests.

STAR Methods

Materials and methods for this manuscript are provided in a separate file.

Figure legends

Figure 1. RipI contributes to virulence in *Ralstonia solanacearum*.

(A and B) Soil drenching inoculation assays in Arabidopsis using *R. solanacearum* GMI1000, a *ripI* mutant (*ΔripI*), and a RipI complementation strain (*ΔripI/ripI*). n=15 plants per genotype. In (**A)** the results are represented as disease progression, showing the average wilting symptoms in a scale from 0 to 4 (mean ± SEM). (**B)** Survival analysis of the data in (A); the disease scoring was transformed into binary data with the following criteria: a disease index lower than 2 was defined as '0', while a disease index equal or higher than 2 was defined as '1' for each specific time point. Statistical analysis was performed using a Log-rank (Mantel-Cox) test, and the corresponding p value is shown in the graph with the same colour as each curve. This experiment was repeated 3 times, and composite data representations are shown in Figure S1C and S1D. **(C)** Growth of *R. solanacearum* GMI1000 WT*, ΔripI*, and *ΔripI/ripI* in tomato stem. Five µL of bacterial suspension (10^6cfu mL^{-1}) were injected into the stem of 4-week-old tomato plants and xylem sap was extracted from each infected plant for bacterial quantification at 2 or 3 dpi (mean ± SEM, n=6 plants per strain). Asterisks indicate significant differences with the GMI1000 strain (* $p<0.05$, *** $p<0.001$, *t*-test). This experiment was performed 3 times with similar results.

Figure 2. RipI associates with plant calmodulins (CaMs) and glutamate decarboxylases (GADs).

(A) RipI-GFP and GFP (as control) were transiently expressed in *N. benthamiana* using *A. tumefaciens* and CaM pull-down was performed using a CaM affinity resin. Immunoblots were analyzed with anti-GFP. **(B)** Co-immunoprecipitation assays to determine interactions between RipI and GADs from *N. benthamiana*, tomato, and Arabidopsis. *A. tumefaciens* containing constructs to express *35S*:*GADs-GFP* and untagged *XVE:RipI* was inoculated in *N. benthamiana* leaves and RipI expression was induced by treatment with 100 µM estradiol 42 hours after infiltration of *A. tumefaciens*. Protein samples were taken 6 hours after estradiol treatment.

Immunoblots were analyzed with anti-GFP and anti-RipI antibodies. **(C)** Interaction between RipI-GFP and GADs-RFP determined by FRET-FLIM upon transient co-expression in *N. benthamiana* leaves. Free RFP was used as a negative control. The accumulation of the independent fluorescent proteins is shown in Figure S4C. Lines represent average values (n=6) and error bars represent standard error. Asterisks indicate significant differences with the RFP control (** $p<0.01$, *** $p<0.001$, *t*-test). In western blot assays, protein marker sizes are provided for reference. These experiments were performed 3 times with similar results.

Figure 3. RipI enhances GABA accumulation in plant cells through promoting CaM binding to GADs.

(A) GFP and RipI-GFP were transiently expressed in *N. benthamiana* using *A. tumefaciens* and GABA content was measured by LC-MS 2 days post-inoculation. The overexpression of AtGAD4 was used as positive control to enhance GABA accumulation, and INF1-GFP was used as control protein to induce immunity-associated cell death. **(B)** CaM affinity pull-down using 12-day-old Arabidopsis transgenic seedlings expressing XVE:RipI. RipI expression was induced with 100 μM estradiol 24 hours before collecting protein samples. Immunoblots were analyzed with anti-RipI and anti-GAD antibodies (see Figure S5). Protein marker sizes are provided for reference. CBB: Coomassie brilliant blue staining for loading control. **(C)** Quantification of CaM-binding GAD protein in (B), relative to Col-0, from three independent experiments. Lines represent average values (n=3) and error bars represent standard error. **(D)** GABA content in *N. benthamiana* plants expressing GFP and RipI-GFP upon VIGS using pTRV2:EV (empty vector control) and pTVR2:*NbCaM2*. VIGS efficiency and protein accumulation are shown in the Fig. S5L and S5M. In (A) and (D), bars represent average values (n=3) and error bars represent standard error. Asterisks indicate significant differences with the GFP control in (A) and with the pTRV2:EV in (D) (* $p<0.05$, *** $p<0.001$, *t*-test). These experiments were performed 3 times with similar results.

Figure 4. *R. solanacearum* can use GABA as a nutrient.

(A) Growth of *R. solanacearum* GMI1000 in minimal medium (MM) with the addition of 5 mM GABA (or water as mock control) as sole nutrient, measured by determining optical density at 600nm. Data points represent average values (n=3) and error bars represent standard error. Error bars are not visible if they are smaller than the data symbol. **(B)** Bacterial quantification from (A), 48 hours post-inoculation. Bars represent average values (n=3) and error bars represent standard error. Asterisks indicate significant differences with the mock control (*** p<0.001, *t*-test). These experiments were performed 3 times with similar results.

Figure 5. Plant GABA contributes to *R. solanacearum* infection.

(A and B) Soil drenching inoculation assays in Arabidopsis Col-0 or the *gad1/2* mutant using *R. solanacearum* GMI1000 (n=15 plants per genotype). In (**A**) the results are represented as disease progression, showing the average wilting symptoms in a scale from 0 to 4 (mean ± SEM). (**B**) Survival analysis of the data in (A); the disease scoring was transformed into binary data with the following criteria: a disease index lower than 2 was defined as '0', while a disease index equal or higher than 2 was defined as '1' for each specific time point. Statistical analysis was performed using a Log-rank (Mantel-Cox) test, and the corresponding p value is shown in the graph with the same colour as each curve. This experiment was repeated 3 times, and composite data representations are shown in Figure S6F and S6G. (**C**) Leaves of four-to-five-week-old Arabidopsis Col-0, *gad1/2*, *siz1-2,* and *NahG* plants were syringe-infiltrated with a bacterial inoculum containing 10^5 cfu mL^{-1} *Pto* DC3000. Four inoculated leaf discs were taken as one sample 3 dpi (mean ± SEM, n=6 plants per genotype, * p<0.05, ** p<0.01, *t*-test). In this experiment, *siz1-2* mutant and *NahG* transgenic line were used as controls to demonstrate that the assay is able to detect enhanced resistance and susceptibility (respectively) to *Pto* DC3000. **(D and E)** Soil drenching inoculation assays in tomato plants with roots containing an empty vector (EV) or an RNAi construct to silence *SlGAD2*. In (**D**) the results are represented as disease progression, showing the average wilting symptoms in a

scale from 0 to 4 (mean ± SEM). (**E**) Survival analysis of the data in (**D**). This experiment was repeated 3 times, and composite data representations are shown in Figure S6K and S6L. **(F)** Wilting symptoms of infected plants in (D). Photos were taken 5 days post-inoculation. **(G and H)** Soil drenching inoculation assays in Arabidopsis Col-0 or the *gad1/2* mutant using *R. solanacearum ΔripI* (n=15 plants per genotype). In (**G**) the results are represented as disease progression, showing the average wilting symptoms in a scale from 0 to 4 (mean ± SEM). (**H**) Survival analysis of the data in (**G**). This experiment was repeated 3 times, and composite data representations are shown in Figure S6M and S6N.

Figure 6. The *R. solanacearum* GABA transaminase GabT contributes to the infection.

(A) Growth of *R. solanacearum* GMI1000 and a *ΔgabT* mutant strain in minimal medium (MM) with the addition of 5 mM GABA (or water as mock control) as sole nutrient, measured by determining optical density at 600nm. Data points represent average values (n=3) and error bars represent standard error. Error bars are not visible if they are smaller than the data symbol. **(B and C)** Soil drenching inoculation assays in Arabidopsis using *R. solanacearum* GMI1000, and a *ΔgabT* mutant strain (n=15 plants per genotype). In (**B**) the results are represented as disease progression, showing the average wilting symptoms in a scale from 0 to 4 (mean ± SEM). (**C**) Survival analysis of the data in (**B**); the disease scoring was transformed into binary data with the following criteria: a disease index lower than 2 was defined as '0', while a disease index equal or higher than 2 was defined as '1' for each specific time point. Statistical analysis was performed using a Log-rank (Mantel-Cox) test, and the corresponding p value is shown in the graph with the same colour as each curve. This experiment was repeated 3 times, and composite data representations are shown in Figure S6P and S6Q. **(D)** Growth of *R. solanacearum* GMI1000 WT and *ΔgabT* in tomato stem. 5 µL of bacterial suspension (10^6 cfu mL^{-1}) were injected into the stem of 4-week-old tomato plants and xylem sap was extracted from each infected plant for bacterial quantification at 2 or 3 dpi. Lines represent average values (n=6

plants per genotype) and error bars represent standard error. These experiments were performed 3 times with similar results. **(E and F)** Soil drenching inoculation assays in Arabidopsis Col-0 or the *gad1/2* mutant using *R. solanacearum ΔgabT* (n=15 plants per genotype). In (**E**) the results are represented as disease progression, showing the average wilting symptoms in a scale from 0 to 4 (mean ± SEM). (**F)** Survival analysis of the data in (E). This experiment was repeated 4 times, and composite data representations are shown in Figure S6R and S6S. In (A) and (D), asterisks indicate significant differences with the GMI1000 strain (* $p<0.05$, *** $p<0.001$, *t*-test).

Figure S1. Characterization of *R. solanacearum* mutant and complementation strains.

(**A and B**) Characterization of the *ΔripI* mutant and complementation strain. (A) Determination of the presence of *ripI* by PCR using a pair of PCR primers that amplify the full-length *ripI* gene or the substitute gentamycin (Gm) resistance cassette, including 500 bp flanking regions. The diagram shows the hybridization sites of the primers used, as well as the fragment sizes. (B) Bacterial growth in nutrient-rich medium was not significantly different among the different strains. GMI1000 WT, *ΔripI,* and the complementation strain (*ΔripI/ripI*) were inoculated into rich BG liquid medium with initial OD_{600}=0.005 and the bacterial growth was monitored at the indicated time points measuring OD_{600} (mean ± SEM, n=3). (**C and D)** RipI contributes to *R. solanacearum* infection in Arabidopsis. Composite data from 3 independent biological repeats (a representative assay is shown in Figure 1A and 1B). All values were pooled together and represented as disease index (C) or percent survival (D). Disease index values represent mean ± SEM (n=45). **(E and F)** Soil-drenching inoculation assay in tomato was performed with GMI1000 WT, *ΔripI* mutant, and RipI complementation strains. n=12 plants per genotype. In (**E**) the results are represented as disease progression, showing the average wilting symptoms in a scale from 0 to 4 (mean ± SEM). (**F**) Survival analysis of the data in (E). This experiment was repeated

3 times. (**G and H)** Composite data from 3 independent biological repeats of the assays shown in (E) and (F). All values were pooled together and represented as disease index (G) or percent survival (H). Disease index values represent mean ± SEM (n=36). For all the survival analyses, the disease scoring was transformed into binary data with the following criteria: a disease index lower than 2 was defined as '0', while a disease index equal or higher than 2 was defined as '1' for each specific time point. Statistical analysis was performed using a Log-rank (Mantel-Cox) test, and the corresponding p value is shown in the graph with the same colour as each curve. **(I and J)** Characterization of the *ΔgabT* mutant. In *R. solanacearum*, *gabT* is a single copy gene. (I) Determination of the presence of gentamycin (*Gm*) by PCR using a pair of PCR primers that amplify a *gabT* promoter fragment or the substitute gentamycin (Gm) resistance cassette. The diagram shows the hybridization sites of the primers used, as well as the fragment sizes.. (e) Bacterial growth in nutrient-rich medium was not significantly different among the different strains. GMI1000 WT and *ΔgabT* were inoculated into rich BG liquid medium with initial OD_{600}=0.005 and the bacterial growth was monitored at the indicated time points measuring OD_{600} (mean ± SEM, n=3).

Figure S2. Identification of RipI interactors.

(A) RipI-GFP interactors identified by immunoprecipitation and LC-MS/MS. The same experiment was performed using free GFP as control. This experiment was performed twice. Only proteins present in both repeats and absent in the GFP control were considered. The table includes the identified proteins, the sequence of the detected peptides, and their respective Mascot ion scores. Only peptides with a Mascot ion score >30 were considered. (**B**) RipI interactors identified by Y2H screening using the *ripI*-encoding fragment (RipI 27-430aa) from GMI1000 as bait. The table includes the gene/protein identifier and the length of the identified fragments. (**C**) Simplified diagram of the involvement of GADs in GABA biosynthesis, including the chemical structures of the reaction substrate and product. **(D)** Phylogenetic analysis of GADs from Arabidopsis, *N. benthamiana*, and tomato, showing protein names and gene/protein identifiers. The protein sequences were obtained from TAIR and

Solgenomics. The phylogenetic tree was generated using the MEGA6 software using the maximum likelihood method.

Figure S3. Transient expression of RipI inhibits the simultaneous expression of other genes using *A. tumefaciens*.

(**A**) When trying to perform targeted co-immunoprecipitation to validate the interaction between RipI and GADs transiently expressed in *N. benthamiana*, we noticed that RipI expression inhibited the simultaneous *A. tumefaciens*-mediated expression of other genes. The gene encoding the beta-glucuronidase (GUS) was used as heterologous gene to analyse transient expression in *N. benthamiana* using *A. tumefaciens*. GUS-FLAG was co-expressed with GFP (control), RipI-GFP, and AtGAD4-GFP (as control protein that enhances GABA accumulation). Western blot using anti-FLAG antibodies shows that co-expression with AtGAD4 compromises the accumulation of GUS-FLAG 1 day post-inoculation (dpi), while the accumulation can be detected to levels similar to the control sample 2 dpi. On the contrary, co-expression with RipI abolished GUS-FLAG accumulation in both time points (marked by red asterisks). Similar results were obtained when co-expressing other genes with RipI in more than three independent experiments. (**B**) RipI expression does not affect the expression of endogenous genes. Given the results shown in (A), to determine if RipI has an effect on genes expressed from the *35S* promoter, RipI-FLAG (or GUS-FLAG as control) was expressed in *N. benthamiana* 16C plants, which constitutively express *35S:GFP* (Ruiz, et al., 1998). At the time point tested (2 dpi), and using the same conditions as in (A), RipI did not cause a reduction in the accumulation of GFP, indicating that RipI does not affect constitutive expression driven by the *35S* promoter. (**C**) RipI inhibits *A. tumefaciens*-mediated gene expression. RNA was extracted from the samples in (A) and qPCR was performed to determine the expression of the *GUS* gene. The *NbEF1a* gene was used to normalize gene expression values. CBB: Coomassie brilliant blue staining for loading control.

Figure S4. RipI interacts with plant GADs.

(**A**) Expression of RipI from an estradiol-inducible promoter. GFP and RipI were expressed under the control of an estradiol-inducible promoter (pXVE) in *N. benthamiana* leaves using *A. tumefaciens*. 100 µM estradiol was infiltrated into leaf tissues 42 hours after infiltration with *A. tumefaciens*, and samples were taken 0, 2, 4, and 6 hours after estradiol infiltration. Proteins were extracted and analyzed by western blot using anti-RipI and anti-GFP antibodies. CBB: Coomassie brilliant blue staining for loading control. **(B)** RipI-MBP associates *in vitro* with AtGAD4-GFP purified from plant cells. GFP and AtGAD4-GFP were expressed in *N. benthamiana* leaves using *A. tumefaciens*. Proteins were purified by GFP immunoprecipitation and incubated with RipI fused to a maltose-binding protein tag (MBP; or MBP-MBP, as control) produced and purified from *E. coli*. After subsequent washes, GFP bound proteins were analyzed by western blot using anti-GFP and anti-MBP antibodies. CBB: Coomassie brilliant blue. **(C)** Accumulation of the fluorescent proteins in the FRET-FLIM assays shown in the Figure 2C, observed using confocal microscopy. All the images were recorded using the same microscope settings.

Figure S5. RipI enhances GABA accumulation.

(**A**) RipI accumulation was analyzed by western blot using an anti-RipI antibody. Arabidopsis Col-0 and two independent transgenic lines expressing RipI from an estradiol-inducible promoter were germinated and grown for 8 days on 1/2 MS plates with or without 10 µM estradiol. (**B**) GABA accumulation was measured in 8 day-old Col-0 WT and RipI#1 seedlings by LC-MS. Three seedlings were used for each measurement (mean ± SEM, n=3, *** $p<0.001$, *t*-test). **(C)** GFP, RipI-GFP, or AtGAD4-GFP were transiently expressed in *N. benthamiana* using *A. tumefaciens* and glutamate content was measured by LC-MS 2 days post-inoculation (mean ± SEM, n=3, ** $p<0.01$, *t*-test). **(D** and **E)** Transient expression of RipI-GFP in *N. benthamiana* **(D)** or tomato **(E)** leaves using *A. tumefaciens* leads to the development of tissue necrosis (dpi, days post-inoculation). (**F and G**) Ion leakage measured in leaf discs taken from *N. benthamiana* (F) or tomato (G) tissues expressing RipI-GFP or GFP (as control), representative of cell death, at the indicated time points. Values

indicate mean ± SEM (n=3 biological replicates, *** p<0.001, **** p<0.0001, *t*-test). (**H**) Phenotypic analysis of Col-0 WT and RipI-expressing seedlings in (**A**). **(I and J)** Transient expression of AtGAD4-GFP in *N. benthamiana* leaves using *A. tumefaciens* does not lead to the development of tissue necrosis (I) (dpi, days post-inoculation) or ion leakage (J). Values indicate mean ± SEM (n=3 biological replicates, **** p<0.0001, *t*-test). (**K**) Characterization of the custom anti-GAD antibody. Total proteins were extracted from 10-day-old Col-0, *gad1*, *gad2*, and *gad1/2* double mutant seedlings growing on 1/2 MS plates, and subjected to western blot analysis using the custom anti-GAD antibody. The two bands observed in Col-0 samples represent endogenous GAD proteins. The result observed in the *gad1/2* double mutant indicates that these bands correspond mostly to GAD1 (approximately 57 kDa) and GAD2 (approximately 56 kDa). Results in single mutant samples indicate that the higher band indeed corresponds to GAD1, while the lower band includes GAD2 and likely other GAD proteins. (**L and M**) Gene silencing of *NbCaM2* by VIGS in *N. benthamiana*, corresponding to the experiment shown in Figure 3D. (**L**) Gene silencing efficiency was verified by qRT-PCR in plants expressing the pTRV2:EV and pTVR2:*NbCaM2* VIGS constructs. RNA was extracted from samples in Figure 3D and qRT-PCR was performed to determine the expression of the *NbCAM2* gene. The *NbEF1a* gene was used to normalize gene expression values (n=3, mean ± SEM). **(M)** Protein accumulation of GFP (as control) and RipI-GFP in plants expressing the pTRV2:EV and pTVR2:*NbCaM2* VIGS constructs. Total proteins from the leaf samples were extracted using protein extraction buffer and subjected to SDS-PAGE. Immunoblots were analyzed with anti-GFP antibody. CBB: Coomassie brilliant blue staining for loading control.

Figure S6. Ralstonia can use GABA as a nutrient during infection.

(A-D) GABA promotes *R. solanacearum* replication in diluted rich medium and tomato xylem sap. (**A**) Growth of *R. solanacearum* GMI1000 in diluted rich medium. *R. solanacearum* was inoculated in 10% complete BG liquid medium with or without 5 mM GABA, with initial OD_{600}=0.005, and bacterial proliferation was monitored at the

indicated time points measuring OD_{600} (mean ± SEM, n=3, *** p<0.001, *t*-test). **(B)** Bacterial quantification 24 hpi in the samples used in (a) (mean ± SEM, n=3, *** p<0.01, *t*-test). **(C)** Growth of *R. solanacearum* GMI1000 in diluted tomato xylem sap (50% tomato xylem sap). *R. solanacearum* was inoculated in 50% tomato xylem sap with or without 5 mM GABA, with initial OD_{600}=0.005 and bacterial proliferation was monitored at the indicated time points measuring OD_{600} (mean ± SEM, n=3, *** p<0.001, *t*-test). **(D)** Bacterial quantification 48 hpi in the samples used in (C) (mean ± SEM, n=3, *** p<0.001, *t*-test). (**E**) GABA accumulation was measured in Arabidopsis Col-0 or the *gad1/2* mutant. Arabidopsis plants were inoculated by soil-drenching using *R. solanacearum* GMI1000 (water was used as mock control), and GABA was measured in the aerial part 3 days post-inoculation (mean ± SEM, n=3, * p<0.05, *t*-test). (**F and G)** *gad1/2* mutant plants display enhanced resistance to *R. solanacearum* GMI1000. Composite data from 3 independent biological repeats (a representative assay is shown in Figure 5A and 5B). All values were pooled together and represented as disease index (F) or percent survival (G). Disease index values represent mean ± SEM (n=45). (**H**) *gad1/2* mutant plants display enhanced resistance to *R. solanacearum* GMI1000. Arabidopsis plants were inoculated by soil-drenching using *R. solanacearum* GMI1000, and bacterial numbers were determined in the aerial part 3 days post-inoculation. Three independent biological repeats were performed (n=6 plants per replicate). Values from all the replicates are represented in this graph; values with the same colour correspond to the same repeat. Horizontal bars represent average values from all the repeats. “Zero” values represent samples where CFU were not detected upon a 1:100 dilution. (**I and J**) RNAi-mediated silencing of *SlGAD2*. (**I**) Expression profile of *GAD* genes in tomato. The GAD gene family contains five members in tomato (Figure S2D). Expression data was retrieved from the tomato eFP Browser (http://bar.utoronto.ca/efp2/Tomato/Tomato_eFPBrowser2.html). Among *SlGAD* genes, *SlGAD2* shows the highest expression in both root and shoot, and was chosen as target for our tomato root RNAi approach. (**J**) RT-PCR analysis to determine the expression of *SlGAD2* in shoot or root tissue of tomato plants with roots transformed

with an empty vector (EV) or an RNAi construct to silence *SlGAD2* (*SlGAD2* RNAi). The tested tissues correspond to the experiment shown in Figure 5. The expression of *SlEF1a* is shown as loading reference. (**K and L)** Tomato plants with reduced expression of *SlGAD2* display enhanced resistance to *R. solanacearum* GMI1000. Composite data from 3 independent biological repeats (a representative assay is shown in Figure 5D and 5E). All values were pooled together and represented as disease index (K) or percent survival (L). Disease index values represent mean ± SEM (n=27). (**M and N)** *gad1/2* mutant plants inoculated with *R. solanacearum ΔripI*. Composite data from 3 independent biological repeats (a representative assay is shown in Figure 5G and 5H). All values were pooled together and represented as disease index (M) or percent survival (N). Disease index values represent mean ± SEM (n=45). (**O**) GABA accumulation was measured in Arabidopsis Col-0 plants inoculated by soil-drenching using *R. solanacearum* GMI1000 or a *ΔripI* mutant (water was used as mock control). GABA was measured in the aerial part 3 days post-inoculation (mean ± SEM, n=3, * $p<0.05$, *t*-test). Three independent biological repeats were performed (n=3 plants per strain per replicate). Values from all the replicates are represented in this graph; values with the same colour correspond to the same repeat. Horizontal bars represent the average values from all the repeats (p-values are shown in the graph, *t*-test). (**P and R**) GabT contributes to *R. solanacearum* infection in Arabidopsis. Composite data from 3 independent biological repeats (a representative assay is shown in Figure 6B and 6C). All values were pooled together and represented as disease index (P) or percent survival (Q). Disease index values represent mean ± SEM (n=45). (**S and T**) *gad1/2* mutant plants inoculated with *R. solanacearum ΔgabT*. Composite data from 4 independent biological repeats (a representative assay is shown in Figure 6E and 6F). All values were pooled together and represented as disease index (R) or percent survival (S). Disease index values represent mean ± SEM (n=60). For all the survival analyses, the disease scoring was transformed into binary data with the following criteria: a disease index lower than 2 was defined as '0', while a disease index equal or higher than 2 was defined as '1' for each specific time point. Statistical analysis was performed

using a Log-rank (Mantel-Cox) test, and the corresponding p value is shown in the graph with the same colour as each curve.

Figure S7. Summary of expression changes in plant *GAD* genes during *RaIstonia* infection from published transcriptomics data.

Expression data of plant *GAD* genes was retrieved from the indicated publications and summarized in this table. In all the reported cases (Hu et al., 2008) (Chen et al., 2014) (Zuluaga et al., 2015) (Wang et al., 2019), the expression of *GAD* genes is up-regulated in compatible interactions (pathogenic strain infecting a susceptible plant) when compared to their expression in incompatible interactions (bacteria inoculated in a resistant plant), suggesting a positive correlation between the success of the infection process and the expression of *GAD* genes.

REFERENCES

Baum, G., Lev-Yadun, S., Fridmann, Y., Arazi, T., Katsnelson, H., Zik, M., and Fromm, H. (1996). Calmodulin binding to glutamate decarboxylase is required for regulation of glutamate and GABA metabolism and normal development in plants. The EMBO Journal *15*, 2988-2996.

Chen, L.Q., Hou, B.H., Lalonde, S., Takanaga, H., Hartung, M.L., Qu, X.Q., Guo, W.J., Kim, J.G., Underwood, W., Chaudhuri, B.*, et al.* (2010). Sugar transporters for intercellular exchange and nutrition of pathogens. Nature *468*, 527-532.

Chen, Y., Ren, X., Zhou, X., Huang, L., Yan, L., Lei, Y., Liao, B., Huang, J., Huang, S., Wei, W.*, et al.* (2014). Dynamics in the resistant and susceptible peanut (Arachis hypogaea L.) root transcriptome on infection with the Ralstonia solanacearum. BMC Genomics *15*, 1078.

Chevrot, R., Rosen, R., Haudecoeur, E., Cirou, A., Shelp, B.J., Ron, E., and Faure, D. (2006). GABA controls the level of quorum-sensing signal in *Agrobacterium tumefaciens*. Proceedings of the National Academy of Sciences *103*, 7460-7464.

Cohn, M., Bart, R.S., Shybut, M., Dahlbeck, D., Gomez, M., Morbitzer, R., Hou, B.-H., Frommer, W.B., Lahaye, T., and Staskawicz, B.J. (2014). *Xanthomonas axonopodis* virulence is promoted by a transcription activator-like effector–mediated induction of a SWEET sugar transporter in cassava. Molecular Plant-Microbe Interactions *27*, 1186-1198.

Cox, K.L., Meng, F., Wilkins, K.E., Li, F., Wang, P., Booher, N.J., Carpenter, S.C.D., Chen, L.-Q., Zheng, H., Gao, X.*, et al.* (2017). TAL effector driven induction of a SWEET gene confers susceptibility to bacterial blight of cotton. Nature Communications *8*, 15588.

Deng, M.-y., Sun, Y.-h., Li, P., Fu, B., Shen, D., and Lu, Y.-j. (2016). The phytopathogenic virulent effector protein RipI induces apoptosis in budding yeast *Saccharomyces cerevisiae*. Toxicon *121*, 109-118.

692 Elphinstone, J.G. (2005). The current bacterial wilt situation: a global overview. . In
693 Bacterial wilt disease and the *Ralstonia solanacearum* species complex, P.P.A.C.H.
694 C. Allen, ed. (St Paul, MN: APS Press), pp. 9–28.
695 Fatima, U., and Senthil-Kumar, M. (2015). Plant and pathogen nutrient acquisition
696 strategies. Frontiers in plant science *6*, 750-750.
697 Genin, S. (2010). Molecular traits controlling host range and adaptation to plants in
698 *Ralstonia solanacearum*. New Phytologist *187*, 920-928.
699 Hu, J., Barlet, X., Deslandes, L., Hirsch, J., Feng, D.X., Somssich, I., and Marco, Y.
700 (2008). Transcriptional responses of *Arabidopsis thaliana* during wilt Disease caused
701 by the soil-Borne phytopathogenic bacterium, *Ralstonia solanacearum*. PLOS ONE *3*,
702 e2589.
703 Kamoun, S., van West, P., Vleeshouwers, V.G.A.A., de Groot, K.E., and Govers, F.
704 (1998). Resistance of *Nicotiana benthamiana* to *Phytophthora infestans* is mediated
705 by the recognition of the elicitor protein INF1. The Plant Cell *10*, 1413-1425.
706 Koike, S., Matsukura, C., Takayama, M., Asamizu, E., and Ezura, H. (2013).
707 Suppression of γ-Aminobutyric Acid (GABA) transaminases induces prominent GABA
708 accumulation, dwarfism and infertility in the tomato (*Solanum lycopersicum* L.). Plant
709 and Cell Physiology *54*, 793-807.
710 Macho, A.P. (2016). Subversion of plant cellular functions by bacterial type-III
711 effectors: beyond suppression of immunity. New Phytologist *210*, 51-57.
712 Macho, A.P., and Zipfel, C. (2015). Targeting of plant pattern recognition
713 receptor-triggered immunity by bacterial type-III secretion system effectors. Current
714 Opinion in Microbiology *23*, 14-22.
715 Mekonnen, D.W., Flügge, U.-I., and Ludewig, F. (2016). Gamma-aminobutyric acid
716 depletion affects stomata closure and drought tolerance of *Arabidopsis thaliana*. Plant
717 Science *245*, 25-34.
718 Park, D.H., Mirabella, R., Bronstein, P.A., Preston, G.M., Haring, M.A., Lim, C.K.,
719 Collmer, A., and Schuurink, R.C. (2010). Mutations in γ-aminobutyric acid (GABA)
720 transaminase genes in plants or *Pseudomonas syringae* reduce bacterial virulence.
721 The Plant Journal *64*, 318-330.

722 Peeters, N., Carrère, S., Anisimova, M., Plener, L., Cazalé, A.-C., and Genin, S.
723 (2013). Repertoire, unified nomenclature and evolution of the Type III effector gene
724 set in the *Ralstonia solanacearum* species complex. BMC Genomics *14*, 859.
725 Ramesh, S.A., Tyerman, S.D., Gilliham, M., and Xu, B. (2017). γ-Aminobutyric acid
726 (GABA) signalling in plants. Cellular and Molecular Life Sciences *74*, 1577-1603.
727 Rico, A., and Preston, G.M. (2008). *Pseudomonas syringae* pv. *tomato* DC3000 uses
728 constitutive and apoplast-induced nutrient assimilation pathways to catabolize
729 nutrients that are abundant in the tomato apoplast. Molecular Plant-Microbe
730 Interactions *21*, 269-282.
731 Ruiz, M.T., Voinnet, O., and Baulcombe, D.C. (1998). Initiation and maintenance of
732 virus-induced gene silencing. The Plant Cell *10*, 937-946.
733 Sabbagh, C.R.R., Carrere, S., Lonjon, F., Vailleau, F., Macho, A.P., Genin, S., and
734 Peeters, N. (2019). Pangenomic type III effector database of the plant pathogenic
735 *Ralstonia* spp. PeerJ *7*, e7346.
736 Schwartz, A.R., Morbitzer, R., Lahaye, T., and Staskawicz, B.J. (2017). TALE-induced
737 bHLH transcription factors that activate a pectate lyase contribute to water soaking in
738 bacterial spot of tomato. Proceedings of the National Academy of Sciences *114*,
739 E897-E903.
740 Shelp, B.J., Bozzo, G.G., Trobacher, C.P., Zarei, A., Deyman, K.L., and Brikis, C.J.
741 (2012). Hypothesis/review: Contribution of putrescine to 4-aminobutyrate (GABA)
742 production in response to abiotic stress. Plant Science *193-194*, 130-135.
743 Snedden, W.A., Koutsia, N., Baum, G., and Fromm, H. (1996). Activation of a
744 recombinant Petunia glutamate decarboxylase by calcium/calmodulin or by a
745 monoclonal antibody which recognizes the calmodulin binding domain. Journal of
746 Biological Chemistry *271*, 4148-4153.
747 Solomon, P.S., and Oliver, R.P. (2002). Evidence that γ-aminobutyric acid is a major
748 nitrogen source during *Cladosporium fulvum* infection of tomato. Planta *214*, 414-420.
749 Subramoni, S., Nathoo, N., Klimov, E., and Yuan, Z.-C. (2014). *Agrobacterium*
750 *tumefaciens* responses to plant-derived signaling molecules. Frontiers in plant
751 science *5*.

Tarkowski, Ł.P., Signorelli, S., and Höfte, M. (2020). γ-Aminobutyric acid and related amino acids in plant immune responses: Emerging mechanisms of action. Plant, Cell & Environment.

Toruño, T.Y., Stergiopoulos, I., and Coaker, G. (2016). Plant-pathogen effectors: cellular probes interfering with plant defenses in spatial and temporal manners. Annual Review of Phytopathology *54*, 419-441.

Wang, G., Kong, J., Cui, D., Zhao, H., Niu, Y., Xu, M., Jiang, G., Zhao, Y., and Wang, W. (2019). Resistance against Ralstonia solanacearum in tomato depends on the methionine cycle and the γ-aminobutyric acid metabolic pathway. The Plant Journal *97*, 1032-1047.

Wang, K., Senthil-Kumar, M., Ryu, C.-M., Kang, L., and Mysore, K.S. (2012). Phytosterols play a key role in plant innate immunity against bacterial pathogens by regulating nutrient efflux into the apoplast. Plant physiology *158*, 1789-1802.

Ward, J.L., Forcat, S., Beckmann, M., Bennett, M., Miller, S.J., Baker, J.M., Hawkins, N.D., Vermeer, C.P., Lu, C., Lin, W.*, et al.* (2010). The metabolic transition during disease following infection of *Arabidopsis thaliana* by *Pseudomonas syringae* pv. *tomato*. The Plant Journal *63*, 443-457.

Xin, X.-F., Nomura, K., Aung, K., Velásquez, A.C., Yao, J., Boutrot, F., Chang, J.H., Zipfel, C., and He, S.Y. (2016). Bacteria establish an aqueous living space in plants crucial for virulence. Nature *539*, 524-529.

Xue, H., Lozano-Durán, R., and Macho, A.P. (2020). Insights into the root invasion by the plant pathogenic bacterium *Ralstonia solanacearum*. Plants *9*, 516.

Yamada, K., Saijo, Y., Nakagami, H., and Takano, Y. (2016). Regulation of sugar transporter activity for antibacterial defense in *Arabidopsis*. Science *354*, 1427-1430.

Zuluaga, A.P., Solé, M., Lu, H., Góngora-Castillo, E., Vaillancourt, B., Coll, N., Buell, C.R., and Valls, M. (2015). Transcriptome responses to Ralstonia solanacearum infection in the roots of the wild potato Solanum commersonii. BMC Genomics *16*, 246.

Zuluaga, A.P., Puigvert, M., and Valls, M. (2013). Novel plant inputs influencing *Ralstonia solanacearum* during infection. Frontiers in Microbiology *4*.

782

783

Figure 1

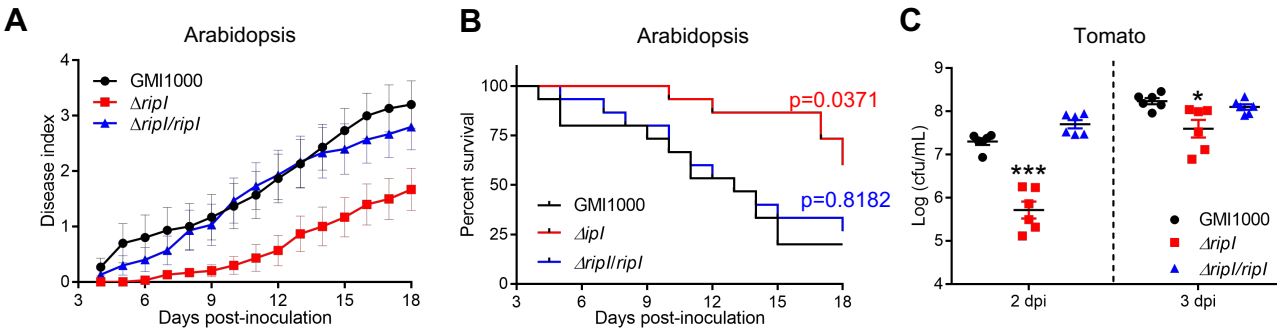

Figure 1. RipI contributes to virulence in *Ralstonia solanacearum*.
(A and B) Soil drenching inoculation assays in Arabidopsis using *R. solanacearum* GMI1000, a *ripI* mutant (*ΔripI*), and a RipI complementation strain (*ΔripI/ripI*). n=15 plants per genotype. In (**A)** the results are represented as disease progression, showing the average wilting symptoms in a scale from 0 to 4 (mean ± SEM). (**B)** Survival analysis of the data in (A); the disease scoring was transformed into binary data with the following criteria: a disease index lower than 2 was defined as '0', while a disease index equal or higher than 2 was defined as '1' for each specific time point. Statistical analysis was performed using a Log-rank (Mantel-Cox) test, and the corresponding p value is shown in the graph with the same colour as each curve. This experiment was repeated 3 times, and composite data representations are shown in Figure S1C and S1D. **(C)** Growth of *R. solanacearum* GMI1000 WT, *ΔripI*, and *ΔripI/ripI* in tomato stem. Five µL of bacterial suspension (10^6cfu mL^{-1}) were injected into the stem of 4-week-old tomato plants and xylem sap was extracted from each infected plant for bacterial quantification at 2 or 3 dpi (mean ± SEM, n=6 plants per strain). Asterisks indicate significant differences with the GMI1000 strain (* p<0.05, *** p<0.001, *t*-test). This experiment was performed 3 times with similar results.

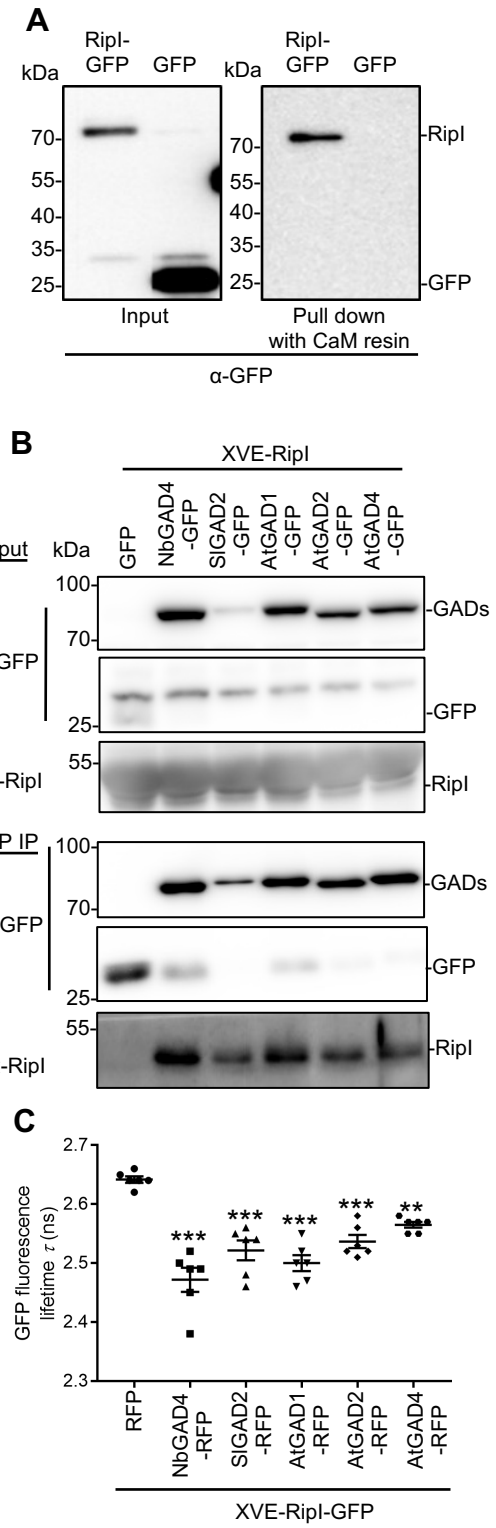

Figure 2. RipI associates with plant calmodulins (CaMs) and glutamate decarboxylases (GADs). **(A)** RipI-GFP and GFP (as control) were transiently expressed in *N. benthamiana* using *A. tumefaciens* and CaM pull-down was performed using a CaM affinity resin. Immunoblots were analyzed with anti-GFP. **(B)** Co-immunoprecipitation assays to determine interactions between RipI and GADs from *N. benthamiana*, tomato, and Arabidopsis. *A. tumefaciens* containing constructs to express *35S:GADs-GFP* and untagged *XVE:RipI* was inoculated in *N. benthamiana* leaves and RipI expression was induced by treatment with 100 µM estradiol 42 hours after infiltration of *A. tumefaciens*. Protein samples were taken 6 hours after estradiol treatment. Immunoblots were analyzed with anti-GFP and anti-RipI antibodies. **(C)** Interaction between RipI-GFP and GADs-RFP determined by FRET-FLIM upon transient co-expression in *N. benthamiana* leaves. Free RFP was used as a negative control. The accumulation of the independent fluorescent proteins is shown in Figure S4C. Lines represent average values (n=6) and error bars represent standard error. Asterisks indicate significant differences with the RFP control (** $p<0.01$, *** $p<0.001$, *t*-test). In western blot assays, protein marker sizes are provided for reference. These experiments were performed 3 times with similar results.

Figure 3

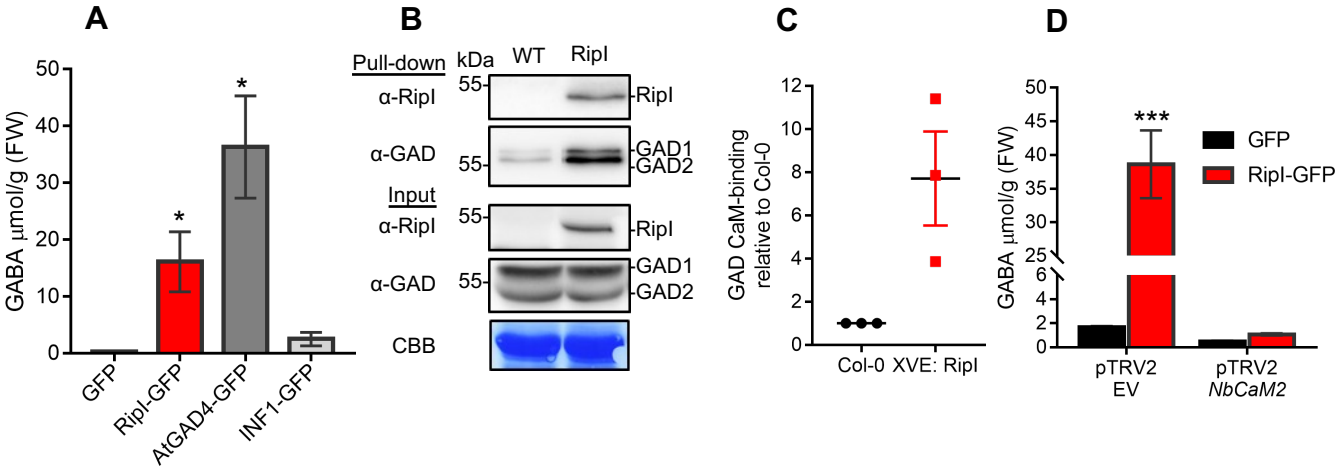

Figure 3. RipI enhances GABA accumulation in plant cells through promoting CaM binding to GADs.

(A) GFP and RipI-GFP were transiently expressed in *N. benthamiana* using *A. tumefaciens* and GABA content was measured by LC-MS 2 days post-inoculation. The overexpression of AtGAD4 was used as positive control to enhance GABA accumulation, and INF1-GFP was used as control protein to induce immunity-associated cell death. **(B)** CaM affinity pull-down using 12-day-old Arabidopsis transgenic seedlings expressing XVE:RipI. RipI expression was induced with 100 µM estradiol 24 hours before collecting protein samples. Immunoblots were analyzed with anti-RipI and anti-GAD antibodies (see Figure S5). Protein marker sizes are provided for reference. CBB: Coomassie brilliant blue staining for loading control. **(C)** Quantification of CaM-binding GAD protein in (B), relative to Col-0, from three independent experiments. Lines represent average values (n=3) and error bars represent standard error. **(D)** GABA content in *N. benthamiana* plants expressing GFP and RipI-GFP upon VIGS using pTRV2:EV (empty vector control) and pTVR2:*NbCaM2*. VIGS efficiency and protein accumulation are shown in the Fig. S5L and S5M. In (A) and (D), bars represent average values (n=3) and error bars represent standard error. Asterisks indicate significant differences with the GFP control in (A) and with the pTRV2:EV in (D) (* $p<0.05$, *** $p<0.001$, *t*-test). These experiments were performed 3 times with similar results.

Figure 4

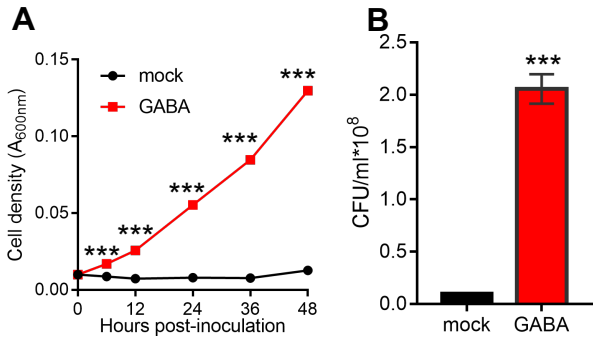

Figure 4. *R. solanacearum* can use GABA as a nutrient.
(A) Growth of *R. solanacearum* GMI1000 in minimal medium (MM) with the addition of 5 mM GABA (or water as mock control) as sole nutrient, measured by determining optical density at 600nm. Data points represent average values (n=3) and error bars represent standard error. Error bars are not visible if they are smaller than the data symbol. **(B)** Bacterial quantification from (A), 48 hours post-inoculation. Bars represent average values (n=3) and error bars represent standard error. Asterisks indicate significant differences with the mock control (*** $p<0.001$, *t*-test). These experiments were performed 3 times with similar results.

Figure 5

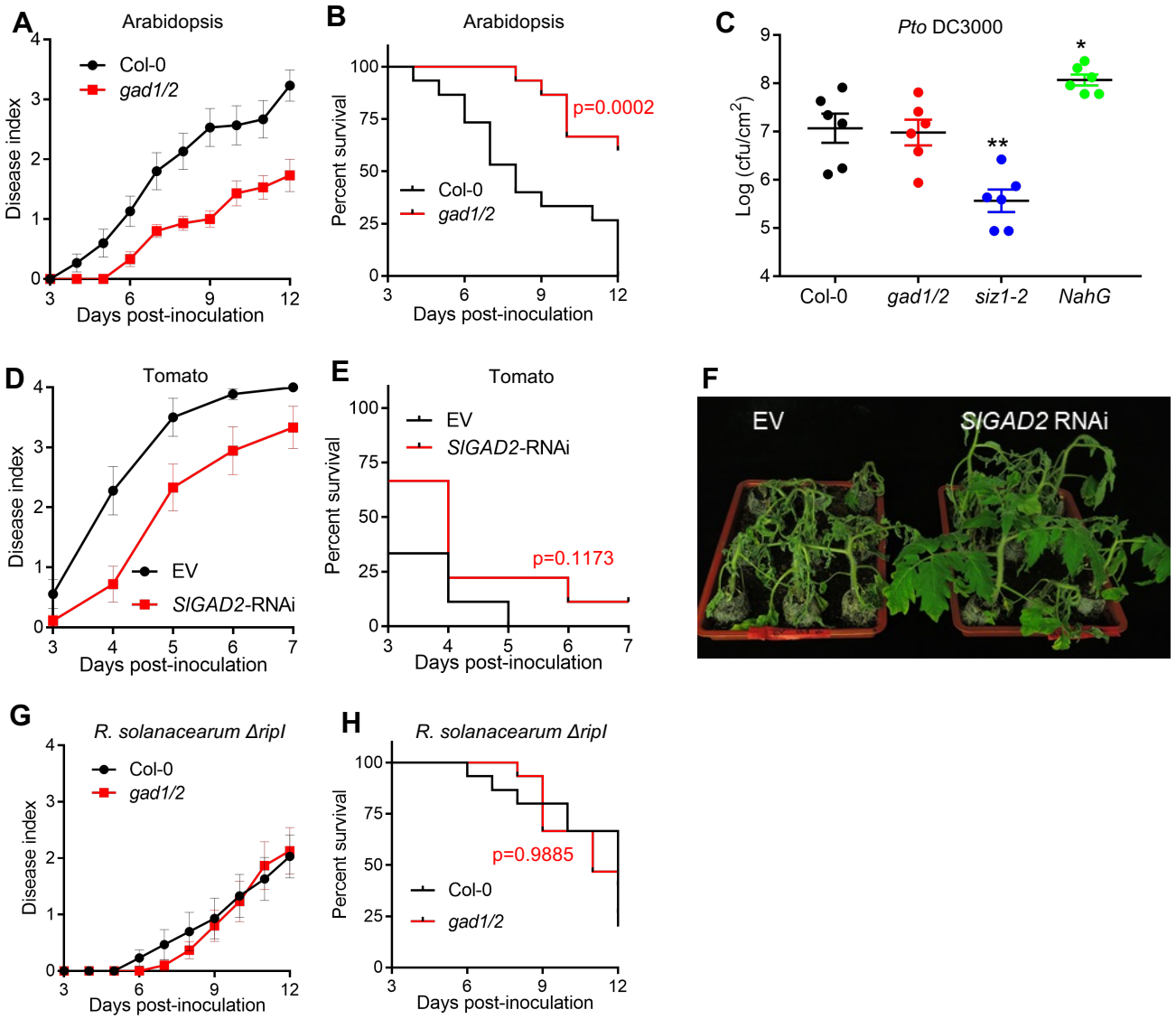

Figure 5. Plant GABA contributes to *R. solanacearum* infection.
(A and B) Soil drenching inoculation assays in Arabidopsis Col-0 or the *gad1/2* mutant using *R. solanacearum* GMI1000 (n=15 plants per genotype). In (**A**) the results are represented as disease progression, showing the average wilting symptoms in a scale from 0 to 4 (mean ± SEM). (**B**) Survival analysis of the data in (A); the disease scoring was transformed into binary data with the following criteria: a disease index lower than 2 was defined as '0', while a disease index equal or higher than 2 was defined as '1' for each specific time point. Statistical analysis was performed using a Log-rank (Mantel-Cox) test, and the corresponding p value is shown in the graph with the same colour as each curve. This experiment was repeated 3 times, and composite data representations are shown in Figure S6F and S6G. (**C**) Leaves of four-to-five-week-old Arabidopsis Col-0, *gad1/2*, *siz1-2,* and *NahG* plants were syringe-infiltrated with a bacterial inoculum containing 10^5 cfu mL^{-1} *Pto* DC3000. Four inoculated leaf discs were taken as one sample 3 dpi (mean ± SEM, n=6 plants per genotype, * p<0.05, ** p<0.01, *t*-test). In this experiment, *siz1-2* mutant and *NahG* transgenic line were used as controls to demonstrate that the assay is able to detect enhanced resistance and susceptibility (respectively) to *Pto* DC3000. **(D and E)** Soil drenching inoculation assays in tomato plants with roots containing an empty vector (EV) or an RNAi construct to silence *SlGAD2*. In (**D**) the results are represented as disease progression, showing the average wilting symptoms in a scale from 0 to 4 (mean ± SEM). (**E**) Survival analysis of the data in (**D**). This experiment was repeated 3 times, and composite data representations are shown in Figure S6K and S6L. **(F)** Wilting symptoms of infected plants in (D). Photos were taken 5 days post-inoculation. **(G and H)** Soil drenching inoculation assays in Arabidopsis Col-0 or the *gad1/2* mutant using *R. solanacearum Δripl* (n=15 plants per genotype). In (**G**) the results are represented as disease progression, showing the average wilting symptoms in a scale from 0 to 4 (mean ± SEM). (**H**) Survival analysis of the data in (**G**). This experiment was repeated 3 times, and composite data representations are shown in Figure S6M and S6N.

Figure 6

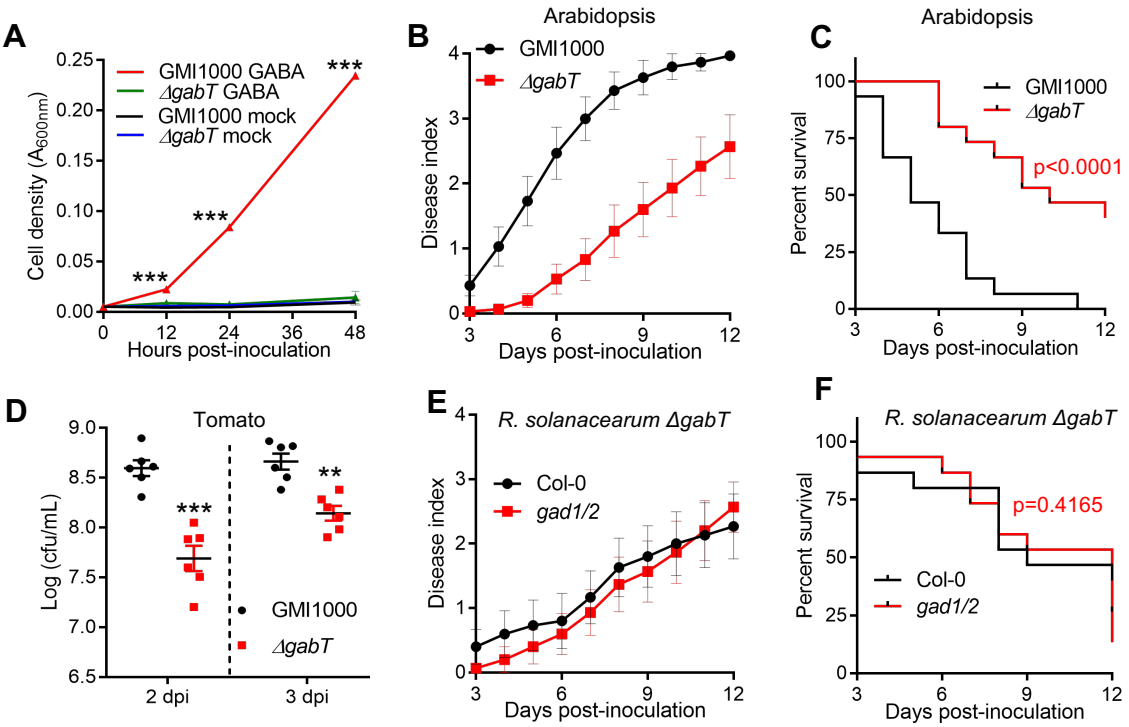

Figure 6. The *R. solanacearum* GABA transaminase GabT contributes to the infection.
(A) Growth of *R. solanacearum* GMI1000 and a *ΔgabT* mutant strain in minimal medium (MM) with the addition of 5 mM GABA (or water as mock control) as sole nutrient, measured by determining optical density at 600nm. Data points represent average values (n=3) and error bars represent standard error. Error bars are not visible if they are smaller than the data symbol. **(B and C)** Soil drenching inoculation assays in Arabidopsis using *R. solanacearum* GMI1000, and a *ΔgabT* mutant strain (n=15 plants per genotype). In (**B**) the results are represented as disease progression, showing the average wilting symptoms in a scale from 0 to 4 (mean ± SEM). (**C**) Survival analysis of the data in (**B**); the disease scoring was transformed into binary data with the following criteria: a disease index lower than 2 was defined as '0', while a disease index equal or higher than 2 was defined as '1' for each specific time point. Statistical analysis was performed using a Log-rank (Mantel-Cox) test, and the corresponding p value is shown in the graph with the same colour as each curve. This experiment was repeated 3 times, and composite data representations are shown in Figure S6P and S6Q. **(D)** Growth of *R. solanacearum* GMI1000 WT and *ΔgabT* in tomato stem. 5 µL of bacterial suspension (10^6 cfu mL^{-1}) were injected into the stem of 4-week-old tomato plants and xylem sap was extracted from each infected plant for bacterial quantification at 2 or 3 dpi. Lines represent average values (n=6 plants per genotype) and error bars represent standard error. These experiments were performed 3 times with similar results. **(E and F)** Soil drenching inoculation assays in Arabidopsis Col-0 or the *gad1/2* mutant using *R. solanacearum ΔgabT* (n=15 plants per genotype). In (**E**) the results are represented as disease progression, showing the average wilting symptoms in a scale from 0 to 4 (mean ± SEM). (**F**) Survival analysis of the data in (E). This experiment was repeated 4 times, and composite data representations are shown in Figure S6R and S6S. In (A) and (D), asterisks indicate significant differences with the GMI1000 strain (* p<0.05, *** p<0.001, *t*-test).